The Toughening Mechanism in a Continuous SiC Fiber/CVI-SiC Matrix Composite

K. W. WHITE*, R. C. BRADT** and A. S. KOBAYASHI**
*College of Engineering, University of Houston, Houston, TX 77204-4792, USA
**College of Engineering, University of Washington, Seattle, WA 9815, USA

ABSTRACT

The R-curve behavior of a continuous SiC fiber reinforced CVI-SiC matrix composite was determined at room temperature, under conditions of stable crack growth. The fracture surface energy was found to increase from an initial value of 1500 J/m^2 to about 5000 J/m^2 over a crack extension of about 1.4 mm. The toughening contribution from the following wake region was deduced from re-notched specimens, where the R-curve of the composite was compared before and after removal of that volume of material immediately behind the primary crack tip. After removal of this following wake region, the crack growth resistance returned to the original value that was obtained at the start of the initial test. Agreement of the two initial values suggests that the stress intensity factor is strongly dependent on the following wake region, and not on the crack length alone. This clearly identifies the SiC fiber bridging across the newly formed crack faces as the mechanism for the dramatic rising R-curve behavior observed in this composite.

KEYWORDS

Ceramics, Composites, Fracture, R-curve, Toughening Mechanisms, Continuous Fiber Reinforcement.

INTRODUCTION

The crack growth resistance for some materials is characterized by an increasing toughness with crack extension, which can be described by a rising R-curve [1]. It indicates the presence of a cumulative toughening mechanism that usually exhibits a strong non-linear character [2-8]. For whisker or fiber reinforced ceramic matrix composites, a mechanism of whisker or fiber bridging across the newly formed crack faces in the following wake region of the advancing primary crack tip has been proposed. This paper addresses that proposition, the role of the following wake region and the crack face bridging phenomena therein. Applying the experimental technique of removing the following wake region by "resawing" an arrested crack that had previously been extended or propagated in a stable fashion, this experiment enables the assessment of the R-curve behavior of the same crack with and without the presence of a following wake region. The results clearly illustrate the paramount role of the following wake

region in the crack growth resistance and rising R-curve behavior.

EXPERIMENTAL PROCEDURES

The material selected for this study offers a pronounced R-curve behavior, with a strong rise in the fracture surface energy during the initial stages of crack extension. It has been previously studied by Pan et. al.[2], who reported on the fracture toughness anisotropy and also described its processing. The material is a SiC/SiC composite which is a 2-D laminate of an 8-harness satin weave of Nicalon fibers in a matrix of chemical vapor infiltrated SiC; the matrix is the cubic (3C) beta form of SiC. This continuous fiber composite has a fiber volume fraction of about 40%, a matrix volume fraction of about 28% and a density of 2.16 g/cm^3. The microstructure is illustrated by the scanning electron micrograph of the fracture surface in Fig. 1, where it is characterized by extensive fiber pullout.

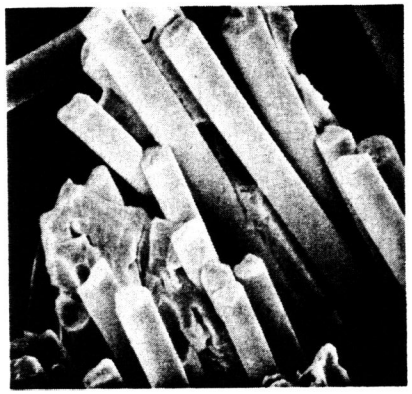

Fig. 1 SEM photograph of the fracture surface of the SiC/SiC continuous whisker composite.

Fracture resistance parameters were evaluated using the straight-notched, three point bend bar configuration, shown in Fig. 2. As the development of stable crack growth is not difficult in this material, the straight-notch configuration was used rather than the chevron-notch, for it offers maximum crack surface area for the evaluation of the crack face bridging mechanism. Machining of the notch with a 0.254 mm thick diamond saw yielded an initial crack of 0.300 mm in width at 56% of the specimen depth.

The crack was initially advanced to a predetermined length as estimated from the compliance, corresponding to a crack depth of about 70% of the specimen width, W. This represents

approximately one half of the initial uncracked ligament. The selection of this crack length allows for adequate crack wake development beyond the maximum applied load, P_{MAX}, in a stable manner, without encroaching on the steepest section of the numerically determined compliance calibration curve.

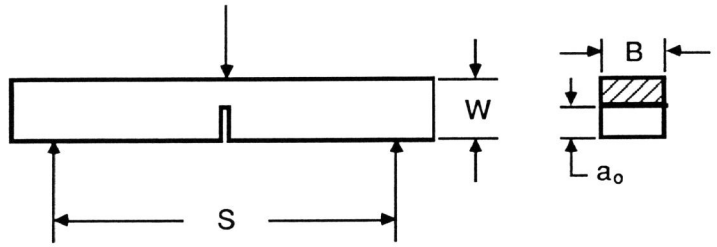

Fig. 2 Schematic representation of the Straight Notch three-point-bend Fracture Specimen Geometry.

The use of this re-notching technique is intended for the identification of the role of the following wake region in the fracture process [9]. By comparing the fracture behavior of the specimen containing a fully developed wake region with a similar specimen with the wake region removed, the contribution from the wake may be evaluated. Fig. 3 schematically illustrates the role of the fiber reinforcement in the fracture process. The re-notching experiment may be visualized as the removal of the bridging fibers from the region following the primary crack tip by diamond sawing. By accurately determining the crack length throughout the fracture experiment, the extending crack may be stopped at any desired point for the mechanical removal of the following wake region.The optimum "re-sawing" depth was estimated to be about 0.2 mm less than the calculated effective crack length, thus preserving the natural crack tip that was developed during the initial segment of the test. The cracked specimen is then placed in a fixture, designed to secure it for re-notching without loading the crack tip. This fixture indexes the same specimen surfaces that were used during the original notching operation, providing accurate alignment of the notch with the path of the circular cutting blade. The same blade (0.254 mm thick by 100 mm diameter with a 220 grit diamond impregnated coating) was used here as in the original notching operation.

The instantaneous stress intensity factor, K_{Ii}, can be evaluated at any point along the load - displacement record from:

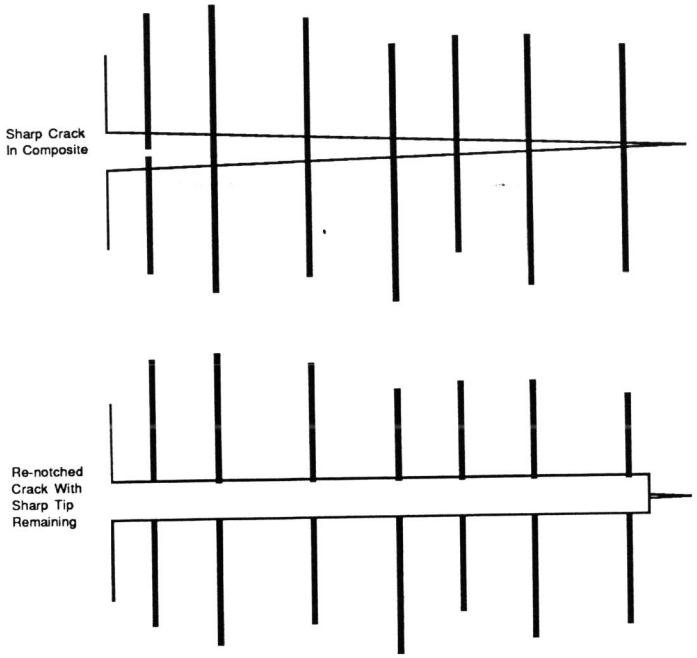

Fig. 3 Schematic of fiber bridging in the following wake region and the re-notching technique.

$$K_{Ii} = \left[\frac{P_i}{B\sqrt{W}}\right] Y_i \qquad (1)$$

where P_i is the corresponding load, B is the specimen thickness, W is the specimen width, and Y_i is the corresponding geometry correction factor. The instantaneous stress intensity factor, K_{Ii} is equal to K_{IC} if $P_i = P_{max}$ and the appropriate geometry correction factor is applied. For flat R-curve materials, exclusive of the present composite, this factor is identical to Y_{MIN}. For the present case, however, the geometry correction factor is obtained through the sequence of calculations depicted graphically in Fig. 4.

The load and displacement information can be combined with the applicable compliance calibration curve to obtain an effective crack length. The instantaneous specimen compliance, C_i, for each point of interest on the load versus load point displacement (LPD) curve is given as:

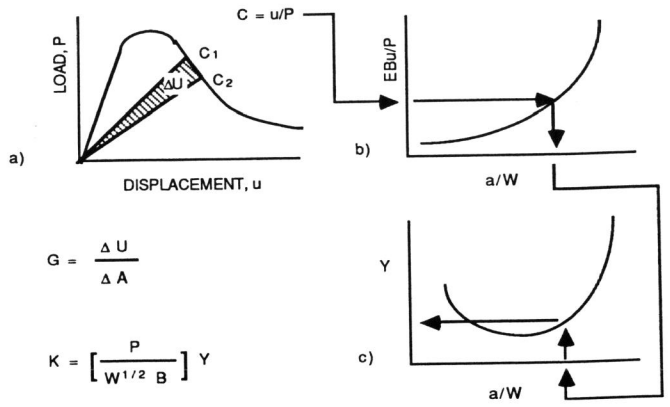

Fig. 4 Schematic of the Calculation Sequence for the Fracture Parameters.

$$C_i = \frac{u_i}{P_i} \qquad (2)$$

where u_i is the instantaneous displacement(in this case LPD) and P_i is the instantaneous load, both taken from the load displacement record, shown schematically in Fig. 4a. The compliance may be normalized as follows:

$$C' = C_i B E' \qquad (3)$$

In this relation the instantaneous dimensionless compliance, C_i', is determined from Equation (2), B is the specimen thickness, and E' is the elastic modulus of the material system under the appropriate state of stress. This dimensionless compliance will then be used to identify the effective crack length at the point of unloading through the numerical relationship shown graphically in Fig. 4b.

Expression (3) can be applied to evaluate the instantaneous effective crack length through the numerically determined compliance calibration curve shown in Fig. 4b. The dimensionless crack length, a/W, obtained in this fashion is then used to evaluate the instantaneous geometry correction factor, Y_i, from the relation shown schematically in Fig. 4c. Both of these curves (Figs. 4b & 4c) were determined numerically for the specific specimen geometry. Therefore, for any given specimen configuration, the stress intensity factor can be calculated from the geometry correction factor, the specimen dimensions and the corresponding load.

The crack growth resistance in terms of the fracture surface energy, G_R, can be readily calculated from the relationship:

$$G_R = \frac{\Delta U_i}{\Delta A_i} \qquad (4)$$

where U_i is the instantaneous fracture energy, evaluated from the area under the load versus load-line displacement curve for the i^{th} increment of crack growth, as illustrated in Fig. 4a. The incremental crack surface area, ΔA_i, is determined directly from the load versus load-line displacement curve using the effective crack length, again, obtained from the compliance calibration curve of Fig. 4b, and the specimen dimensions.

RESULTS AND DISCUSSION

The load versus load-line displacement, P-u, record illustrated in Fig. 5 includes the P-u data generated during the extension of both the original crack and the "resawn" crack. Of significance in this figure is that the load for crack re-initiation is only about 50% of final load experienced during the initial segment of the test, once the following wake is removed. This clearly demonstrates that those fibers which were removed from the following wake region by the re-notching procedure supported about 50% of the load. The role of the following wake region in this material is supported by the change in the compliance following the removal of the wake. A comparison of the compliance of the unloading trace with that of the reloading curve shows that the specimen compliance increase resulted from the removal the following wake region. It is evident that the fiber bridging in this region carried a significant portion of the load, and that the specimen behaved as though the crack was significantly shorter than its true length.

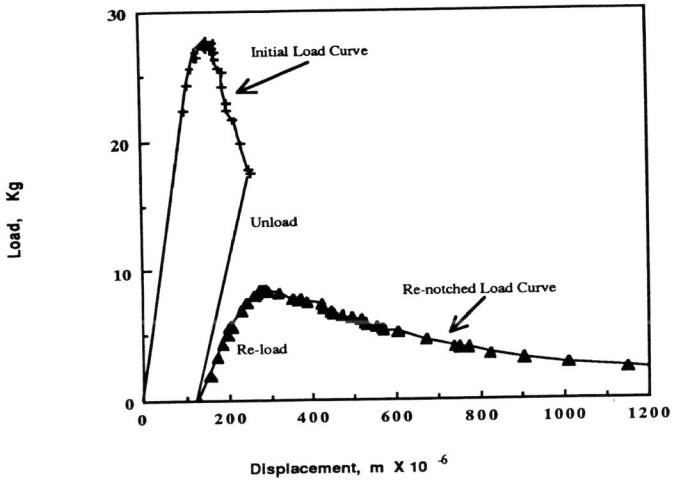

Fig. 5 Load - Displacement Diagram for both the original and the re-notched tests.

The crack growth resistance curves before and after the re-notching process are depicted collectively in Fig. 6. The crack growth resistance in terms of fracture surface energy, G_R, is

observed to increase with crack extension from about 1,500 J/m^2 to about 5,000 J/m^2. This toughening occurs over a crack extension from a/W =56% to a/W=77%, about 1.4 mm, at which point the load was removed to halt the test at the predetermined compliance for the re-notching operation. Upon restarting of the test at the same crack length, and without the benefit of the following wake region, an instantaneous fracture surface energy value of about 1600 J/m^2 is observed. This is within the experimental error of that obtained at the beginning of the test at a/W = a_0/W. At this point, the crack length is nearly identical to that at the completion of the first loading segment, yet the fracture resistance is only one third of the value prior to the following wake region removal. Continuing the test, the resistance to crack extension again increases with increasing crack length as a new following wake region develops. The rapid increase in fracture surface energy at large crack lengths is probably related to a hinging effect as the crack approaches the back surface of the specimen.

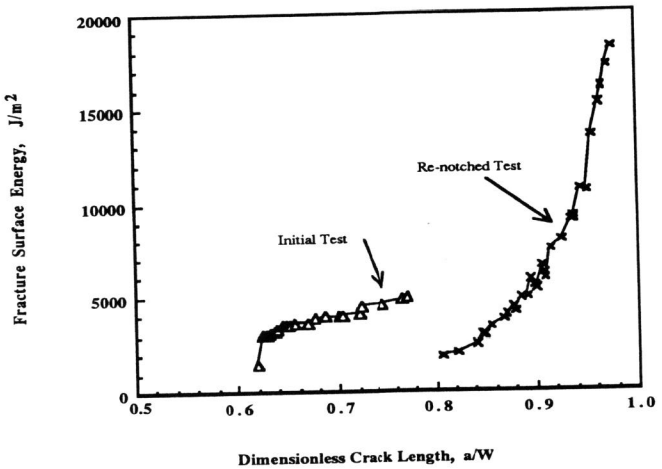

Fig. 6 Fracture Energy, G_R-curve for the combined fracture test. Showing the return the initial fracture energy after removal of the following wake region.

The toughening of this continuous fiber reinforced ceramic matrix composite has been demonstrated to rely principally on the development of a following wake region behind the primary crack tip. In evidence, the fracture surface energy increases significantly with crack extension over the initial portion of the test, until removal of the material behind the crack tip causes the fracture surface energy to return to its original value at the initial conditions. The mechanism responsible for this observed phenomenon involves bridging of the crack faces by microstructural features in the following wake region of the crack, causing a reduction of the crack tip stress intensity factor. As the crack advances, the length of the following wake region increases, providing additional cumulative loading paths to modify the stress environment at

the primary crack tip. As the contribution to the crack growth resistance increases, the material appears to continually toughen, even for large crack lengths. This mechanism is illustrated schematically in Fig. 3, where the fibers serve to bridge the crack faces, somewhat analogous to that of large grains in the monolithic materials [9]. This mechanism is evident from the frequent observation of long pulled-out fibers as depicted in the fracture surface of Fig. 1. The dramatically higher fracture surface energies associated with this composite are easily attributed to the large pullout lengths, and the correspondingly large COD values over which the crack face bridging mechanism may operate.

The extracting fibers of this composite provide much larger surface areas and operate over larger COD's, and hence a larger wake region, when compared with the microstructural features of monolithic ceramic materials. The estimated COD value ($K_{IC}^2/(E\sigma_y)$) for monolithic Al_2O_3 is about 0.1 μm, while that for the present material is about one order of magnitude larger. Therefore, the magnitude of the fracture surface energy and the rise of the R-curve both significantly exceed those of the monolithic materials cited in the literature[9-11], where it is the grain morphology which has a dominant effect on the wake mechanism.

SUMMARY AND CONCLUSIONS

Crack growth resistance curves were determined for a continuous SiC fiber reinforced, CVI-SiC matrix composite (CMC). A strongly rising R-curve observed in this study suggests the intervention of a non-linear toughening mechanism, associated with this microstructure. Re-notching, to remove the following wake region behind the primary crack tip, conclusively proved that the cumulative toughening mechanism is that of fiber bridging of the newly formed crack surfaces in the following wake region. The successful contribution of the fiber bridging mechanism is directly related to the small COD's, with respect to the size of the microstructure, which these materials exhibit during crack growth.

ACKNOWLEDGEMENTS

This research was supported by the Department of Energy under DOE contract number 86A-00209C.

REFERENCES

1] Broek, D., Elementary Engineering Fracture Mechanics, M. Nijoff, The Hague, (1982).

2] Pan, Y.M., Sakai, M., Warren, J.W., and Bradt, R.C., "Toughness Anisotropy for SiC/SiC Laminar Composites," p.631-38, in: Tailoring Multiphase and Composite Ceramics, T.E. Tressler, et al.eds., Plenum (1986).

3] Becher, P.F., Tiegs,T.N., Ogle, J.C., Warwick,W.H., "Toughening of Ceramics By Whisker Reinforcement," in: Fracture Mechanics of Ceramics, R.C. Bradt, et. al. eds., Vol. 7, 61-73, (1986).

4] Tiegs,T.N. and Becher, P.F., "Sintered Al_2O_3-SiC-Whisker Composites," Am. Ceram. Soc. Bull., **66** [2] 339-42, (1987).

5] Lundberg, R., Kahlman, L., Pompe, R., Carlsson, R., Warren, R.,"SiC-Reinforced Si_3N_4 Composites," Am. Ceram. Soc. Bull., **66** [2] 330-33, (1987).

6] Jenkins,M.G., Kobayashi, A.S., White, K.W., Bradt,R.C., "Crack Initiation and Arrest in a SiC Whisker/Al_2O_3 Matrix Composite," J. Amer. Ceram. Soc.,**70** [6] 393-95(1987).

7] Marshall, D.B., Evans, A.G.,"Failure Mechanisms in Ceramic-Fiber/Ceramic-Matrix Composites," J.Amer. Ceram. Soc., **68** [5] 225-231, 1985.

8] Becher, P.F., Wei, G.C.,"Toughening Behavior in SiC-Whisker-Reinforced Alumina," Communications in J. Amer. Ceram. Soc.,**67** [12] C 267-269 (1984).

9] Knehans,R., Steinbrech,R., "Memory Effect of Crack Resistance During Slow Crack Growth in Notched Al_2O_3 Bend Specimens", J. of Mater. Sci. Let.,**1** [8].327-329,(1982).

10] Steinbrech,R., Knehans,R., Schaarwachter,W., "Increase of Crack Resistance During Slow Crack Growth in Al_2O_3 Bend Specimens," J. Mat. Sci.,**18**,pp.265-270 (1983)

11] Swanson, P.L., Fairbanks, C.J., Lawn, B.R., Mai, Y-W.,"Crack-Interface Grain Bridging as a Fracture Resistance Mechanism in Ceramics: I, Experimental Study on Alumina," J.Am. Ceram. Soc. **70**[4] 279-89 (1987).

12] Jenkins,M.G., Kobayashi, A.S., White, K.W., Bradt,R.C., "Finite Element Analysis of The Chevron-Notched, Three-Point Bend Fracture Specimen", International J. of Fracture, **34**, 281-95 (1987).